ChemComm

γ-Agostic Interactions in (MesCCC)Fe-Mes(L) Complexes

SCHOLARONE™
Manuscripts

Journal Name

COMMUNICATION

ROYAL SOCIETY OF CHEMISTRY

γ-Agostic Interactions in (MesCCC)Fe-Mes(L) Complexes

Daniel C. Najera, [a] Marconi N. Peñas-Defrutos,[b,c] Max García-Melchor,[b,*] and Alison R. Fout [a,*]
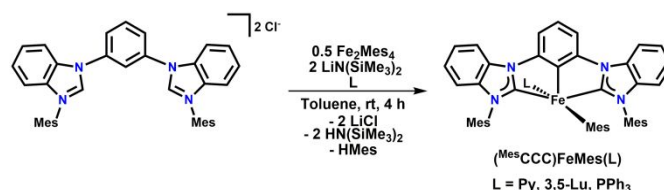
Agostic interactions were observed in the bound mesityl group in a series of iron compounds bearing a bis(NHC) pincer CCC ligand. The L-type ligand on [(CCC)Fe^{II}Mes(L)] complexes influences the strength of the agostic interaction and is manifested in the upfield shift of the ^{1}H NMR resonance for the mesityl methyl resonances. The nature of the interaction was further investigated by density functional theory calculations, allowing to rationalize some unexpected trends and proving to be a powerful predictive tool.

Agostic interactions play a significant, if not decisive, role in the activity of transition metal complexes towards important transformations. This type of interaction is characterized by close intramolecular contacts between the metal and a C–H bond ranging from 1.8 to 2.3 Å for H and relatively small M···H–C angles (i.e. 90 to 140°), concomitant with an upfield shift of the corresponding proton resonance in the ^{1}H NMR spectrum.[1] Beyond their fundamental significance to understanding the nature of chemical bonding, agostic interactions are important in catalyst design due to the stabilization imparted on transition states or key intermediates in organometallic reactions such as β-hydride elimination,[2] olefin polymerization,[3] and C–H activation.[4]

Our groups have a continued interest in exploring the chemistry of first-row transition metal complexes featuring strongly donating, monoanionic, bis(NHC) pincer CCC ligands. Metalation of the CCC ligand framework with late first-row transition metals is often unpredictable and requires metal- and ligand-specific conditions. For example, the metalation of the ^{DIPP}CCC ligand platform (^{DIPP}CCC = bis(2,6-diisopropylphenylbenzimidazol-2-ylidene)phenyl) has been

achieved via: (1) oxidative addition of the aryl C-H bond on a Ni^0 source;[5] (2) *in-situ* deprotonation of the benzimidazolium precursor with Co(N(SiMe$_3$)$_2$)$_2$(Py)$_2$;[6] and (3) reduction of a zwitterionic Fe^{II} intermediate.[7] Conversely, the metalation of the ^{Mes}CCC ligand variant (^{Mes}CCC = bis(2,4,6-trimethylphenylbenzimidazol-2-ylidene)phenyl) has only been achieved with cobalt via route (2).[6] In search of a convenient one-pot metalation with iron through the *in situ* deprotonation of the ligand salt, herein we report the synthesis of a family of (^{Mes}CCC)FeMes(L) complexes featuring a Fe···H–C$_{Mes}$ agostic interaction of tunable strength influenced by the identity of the ligand L.

Tetramesityl diiron(II) (Fe$_2$Mes$_4$) is a convenient source of Fe^{II} which features internal base equivalents and readily forms Lewis base adducts (FeMes$_2$(L)$_2$).[8] These characteristics make it a powerful reagent, and consequently, it has seen increasing application in the deprotonation and metalation of NHC-based ligands.[9] The addition of *in situ* generated FeMes$_2$(Py)$_2$ (Mes = mesityl and Py = pyridine) to a mixture of the ligand salt [H$_3$(^{Mes}CCC)]Cl$_2$ and 2 equiv. of LiN(SiMe$_3$)$_2$ in toluene resulted in the formation of the product (^{Mes}CCC)FeMes(Py) (**1-Py**), which was isolated as a purple powder after workup in 94% yield (Scheme 1). Characterization by ^{1}H NMR spectroscopy revealed a diamagnetic, C_s-symmetric complex with three singlets integrating to 6H each, located at 2.14, 1.45, and 1.16 ppm, assigned to the methyl groups on the flanking mesityl moieties of the ligand (Figure S1). The presence of a second set of three singlets at 2.29, 0.92, and –0.55 ppm, each integrating to 3H, is consistent with retention of a mesityl ligand bound to

[a.] School of Chemical Sciences, University of Illinois at Urbana-Champaign, 600 S. Mathews Ave., Urbana, Illinois 61801, USA. E-mail: fout@illinois.edu

[b.] School of Chemistry, CRANN and AMBER Research Centres, Trinity College Dublin, College Green, Dublin 2, Ireland. Email: garciamm@tcd.ie

[c.] Universidad de Valladolid, Valladolid, Spain.

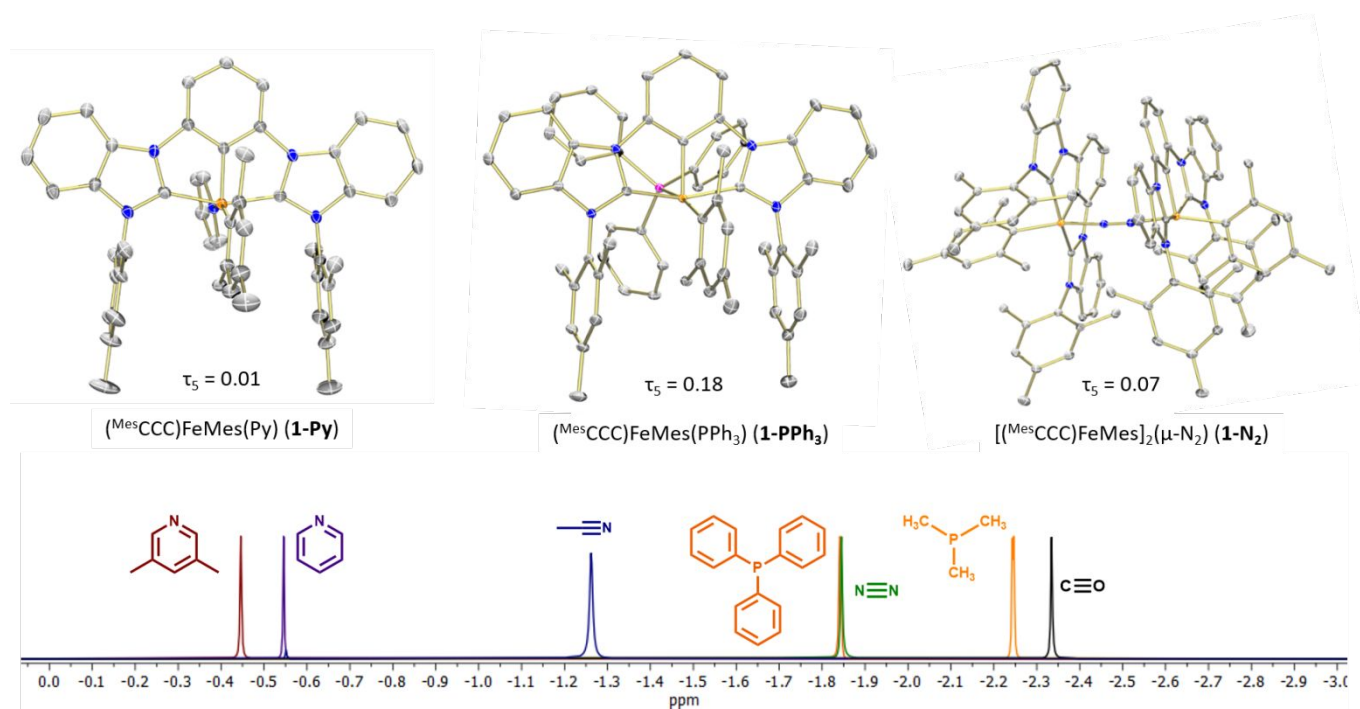**Scheme 1.** Synthesis of **1-Py**, **1-Lu**, and **1-PPh$_3$**.

Figure 1. Top panel: Molecular structures of **1-L** (L = Py, PPh₃ and N₂) with 50% probability ellipsoids. Solvent molecules and hydrogen atoms have been omitted for clarity. Bottom panel: ¹H NMR spectral overlay of the agostic signal in **1-L** complexes using benzene-d_6 as solvent.

iron with restricted rotation about the Fe–C$_{Mes}$ axis, likely due to the steric imposition of the ^{Mes}CCC ligand. The significant upfield shift of the resonance at –0.55 ppm (from 2.16 ppm for free mesitylene in C₆D₆) suggests close proximity between these protons and the Fe center and the presence of an agostic interaction.

Further characterization by single crystal X-ray diffraction studies confirmed the structure of the product (Figure 1). For **1-Py**, this consists of in a formally pentacoordinate, square pyramidal (τ_5 = 0.01)[10] Fe^{II} complex with the Mes and Py ligands in a *trans* disposition (see Tables S3 and S4 for relevant crystallographic distances). The Mes ligand is oriented nearly perpendicular to the plane of the CCC scaffold as a result of steric repulsion from the flanking aryl groups on the ligand. The Fe···C distance between Fe and the *ortho*-methyl group of the Mes ligand (2.703(3) Å) suggested the presence of a Fe···H–C$_{Mes}$ agostic interaction. While reports of C–H agostic interactions at Fe^{II} are numerous, this is a rare example of an aryl γ-agostic complex at iron.[11]

With this synthetic protocol established, we examined the flexibility of this metalation strategy through the synthesis of other (^{Mes}CCC)FeMes(L) complexes and the effect on the agostic interaction (see SI for details). Metalations substituting pyridine for 3,5-lutidine (3,5-Lu) or PPh₃ resulted in the analogous products (^{Mes}CCC)FeMes(3,5-Lu) (**1-Lu**) and (^{Mes}CCC)FeMes(PPh₃) (**1-PPh₃**). The ¹H NMR spectra of **1-Lu** and **1-PPh₃** exhibit the same pattern of two sets of three singlets in the alkyl region observed for **1-Py** (Figures S3, S5). The lutidine methyl protons in **1-Lu** appear as an additional singlet integrating to 6H, showing that the restricted rotation of the Mes ligand is dictated by the presence of *ortho* substituents on the aryl ligand.[12] Notably, the chemical shift of the agostic

methyl group shifted slightly for **1-Lu** at –0.45 ppm, while for **1-PPh₃** it shifted significantly at –1.84 ppm (Figure 1) with weak $J_{P–H}$ coupling (1.3 Hz) observed. Addition of acetonitrile to **1-Py** led to an immediate color change to burgundy. The ¹H NMR spectrum revealed the product as (^{Mes}CCC)FeMes(NCMe) (**1-NCMe**) (Figure S8). Likewise, addition of PMe₃ to **1-Py** resulted in the clean conversion to (^{Mes}CCC)FeMes(PMe₃) (**1-PMe₃**) which displayed the strongest agostic interaction as evidenced by the significant shift of the corresponding resonance in the ¹H NMR spectrum to –2.25 ppm and a larger $J_{P–H}$ = 2.1 Hz comparing to **1-PPh₃** (Figure 1).

Treatment of **1-Py** with BPh₃ to promote N₂ binding yielded a diamagnetic complex featuring an agostic resonance at –1.85 ppm in the ¹H NMR spectrum. Interestingly, the alkyl region featured 8 singlets integrating to 6H each, indicating that the C$_s$ symmetry of the ^{Mes}CCC ligand was broken. While thermally unstable, the addition of pyridine cleanly furnished **1-Py**, negating potential C–H activation of the ligand. Single crystal X-ray diffraction studies revealed a dimeric species consisting of two (^{Mes}CCC)FeMes units bridged by an unactivated dinitrogen ligand (1.135(2) Å, [(^{Mes}CCC)FeMes]₂(μ-N₂) (**1-N₂**)).

Overall, the molecular structures of **1-L** (Figures 1 and S20) exhibited identical features, namely, a pentacoordinate square-pyramidal geometry about iron with the Mes and L-type ligands *trans* to each other. The Fe···C$_{Mes}$ distances ranged from 2.7238(19) Å for **1-Lu** to 2.6456(13) Å for **1-PMe₃**, and correlated well with the shift of the agostic resonance in the ¹H NMR spectra (Figure 1). Interestingly, the experimentally observed trend does not correlate with the donor capability of the pendant ligand nor with its steric bulk. However, it is hinted that it is tightly related with the strength of the agostic interaction. To rationalize the intriguing chemical shifts

observed in the ^{1}H NMR spectra, we performed density functional theory (DFT) calculations in implicit benzene (solvent used to record the NMR spectra) at the ωB97x-D level (see ESI for details). As seen in Table 1, the computed chemical shifts are in excellent agreement with the experimental values, with deviations within 0.5 ppm. In general, the experimental trend is captured by DFT calculations, except for **1-PPh₃** when compared to **1-NCMe**. However, the trend is preserved when comparing the calculated shifts for the specific H involved in the agostic interaction instead of the averaged values of the H atoms in the CH₃ group (*i.e.* −4.38 ppm for PPh₃ vs −4.28 ppm for NCMe).

More interestingly, we found an excellent linear correlation between the optimized Fe···H distance and the experimental shifts (Figure S21), indicating that the shortening of the agostic interaction clearly contributes to the shielding of the corresponding NMR signal. We acknowledge that other factors[13] might be at play, but since all the complexes studied in this work belong to the same family (with negligible geometric variations), we can conclude that the Fe···H distance and the observed NMR shifts are strongly correlated. Specifically, the computed Fe···H distance is *ca.* 0.15 Å shorter for **1-PMe₃** than for **1-Lu**, which causes a *ca.* 1.8 ppm upfield shift. The strengthening of the agostic interaction also leads to the lengthening of the C–H$_{agostic}$ bond, as shown in Table 1. Even though the absolute variation of the sigma C–H bond is minute (*ca.* 0.01 Å) compared to the non-covalent Fe···H (distances well above the sum of covalent radii),[14] the trend is evident. It is also worth noting that the Fe···H distances and Fe···H–C angles reported in Table 1 for all the complexes studied herein are within the range of reported agostic interactions.[15]

Further insight was provided by the non-covalent interaction (NCI) analysis depicted in Figure 2a.[16] This revealed that the strongest attractive NCI corresponds to the agostic bond, while the main repulsive NCI stems from the interaction between the Fe center and the C atom bound to the agostic H. The latter can be better visualized in the inset, which displays the isosurfaces of both interactions restricted to the specific peaks, maintaining their colors. Notably, the computed NCIs for **1-Lu** (Figure S22) indicated a weaker Fe···H interaction compared to **1-PMe₃**, attending to the maximum of the agostic peak. However, to quantify the relative strength of this interaction in the studied complexes we resorted to other analyses, as detailed below.

Natural bond orbital (NBO) and second order perturbation theory (SOPT) analyses revealed that the main donor-acceptor interaction involved in the Fe···H bond concurs in all complexes.

More specifically, the highest ΔE$_{SOPT}$ values were observed for the donation from the bonding orbital (BD) of the C–H bond into the antibonding orbital (BD*) of the Fe–C$_{trans}$, which is mainly constituted by *d* electron density from the Fe center (see Figure
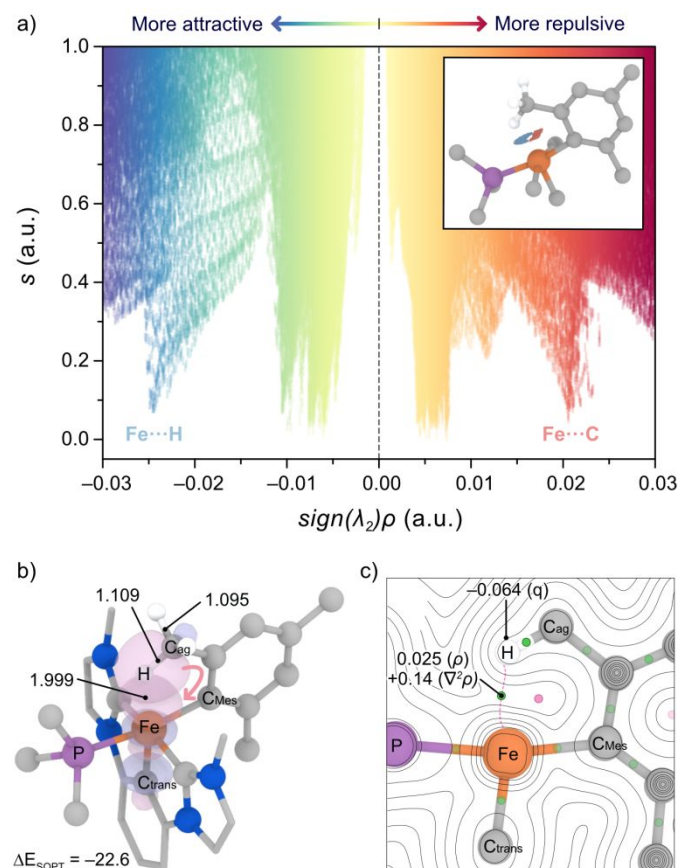
2b for **1-PMe₃**, full details are provided in the ESI).

Figure 2. a) NCI plot for **1-PMe₃**, representing the reduced density gradient, *s*, as a function of the electron density *ρ* multiplied by the sign of the second eigenvalue of the Hessian matrix, $sign(λ_2)ρ$, which effectively displays NCIs as distinct peaks (see ESI for more details). Colder/warmer colors depict attractive/repulsive interactions. Isosurfaces (isovalue = 0.3 a.u) for the most relevant interactions are shown in the inset. b) Selected donor-acceptor NBO interaction (isosurface = 0.07 a.u) for **1-PMe₃**. The ΔE$_{SOPT}$ value (in kcal/mol) and relevant distances (in Å) are provided. Some H atoms have been omitted, while the chelating ligand has been simplified for clarity. c) Electron density map along the Fe···H–C plane obtained by QTAIM. Green/pink dots denote bond/ring critical points, respectively. Values of the $ρ(r)$ and $∇^2ρ(r)$ at the Fe···H bond critical point, as well as the H$_{agostic}$ AIM charge (*q*), are also given in a.u.

Table 1. Computed data related with the C–H···Fe interactions. Data is presented following the experimental chemical shifts to better visualize trends. Calculated chemical shifts are averaged over the three hydrogen atoms in the agostic methyl group and referenced to the shift computed for SiMe₄ using the same methodology (see ESI for more details).

Ligand	Chemical Shift		Geometry Optimization		NBO Analysis		QTAIM Analysis	
	δ$_{exp}$ (ppm) ^{1}H NMR	δ$_{calc}$ (ppm) ^{1}H NMR	Fe···H (Å) H = agostic	C–H (Å) H = agostic	ΔE$_{SOPT}$ (kcal/mol) σCH →Fe[b]	Occupancy (e⁻) BD C–H	ρ(r) Fe···H BCP	ρ(r) C–H BCP
Lu	−0.45	−0.28	2.141	1.103	−10.7	1.959	0.021	0.268
py	−0.55	−0.36	2.117	1.103	−11.6	1.957	0.021	0.267
NCMe	−1.26	−1.70	2.057	1.106	−18.8	1.951	0.021	0.263
PPh₃	−1.84	−1.56	2.027	1.107	−19.3	1.945	0.025	0.264
μ-N₂[a]	−1.85	−2.11	2.019	1.107	−21.6	1.944	0.025	0.262
PMe₃	−2.25	−2.54	1.999	1.109	−22.6	1.941	0.025	0.261
CO	−2.33	−2.73	1.986	1.110	20.3	1.936	0.027	0.260

[a] Averaged values between the agostic interactions involving both metal atoms. [b] The acceptor orbital is a BD* Fe–C, mainly located on the Fe center.

Another clear trend from Table 1 is that the stronger the donor-acceptor NBO interaction (higher ΔE_{SOPT}), the more negative the shift. This prompted us to find an additional linear correlation (Figure S21) by plotting the electron occupancy of the donor NBO against the experimental NMR shift, indicating that the weakening of the C–H bond concomitantly strengthens the Fe···H interaction. Furthermore, we noted that in all our complexes the backdonation (with the BD* C–H orbital as acceptor) is substantially smaller (≤20%) than the donation (see Table S7 for details), which is a common feature in agostic interactions that contrasts with the anagostic ones.[16]

Topology analyses using Quantum Theory of Atoms in Molecules (QTAIM) allowed us to uphold all the stated above.[17] In particular, the generated electron density maps featured a bond critical point (BCP) for the agostic interactions (green dot in Figure 2c), finding that the electron density (ρ) at the Fe···H and C–$H_{agostic}$ BCPs (see Table 1) is tightly and oppositely related; the higher the former the lower the latter. On the other hand, the computed Laplacian of the electron density ($\nabla^2\rho(r)$) was found to be small and positive for Fe···H while high and negative for C–H, which is typical for NCIs and covalent interactions, respectively. Moreover, the AIM charge on the $H_{agostic}$ resulted negative (see Table S10 for additional data), while positive values were found for $H_{anagostic}$.[18]

Finally, DFT predicted that a putative CO derivative would afford the shortest Fe···H distance of 1.986 Å and most upfield ^{1}H NMR resonance. Preparation of the carbonyl species (**1-CO**) confirmed that the agostic signal is the most shielded at −2.33 ppm. However, like other FeMes(CO) complexes, **1-CO** readily undergoes insertion to furnish the acyl complex (^{Mes}CCC)Fe(CO)$_2$(COMes) (**2**) in a CO atmosphere (see ESI for details).[19] NBO analysis on **1-CO** revealed an additional backdonation with important contribution of the CO ligand located *cis* (Figure S23),[20] which further contributes to the weakening of the C–H bond, thus increasing its subsequent reactivity as observed in experiments.

In conclusion, the L-type ligand on [(CCC)Fe^{II}Mes(L)] complexes, influences the strength of the agostic interaction which appears in the upfield shift of the ^{1}H NMR resonance for the mesityl methyl. DFT calculations probed the nature of the interaction and rationalized some unexpected trends.

Conflicts of interest

The authors have no conflicts to declare.

Notes and references

1   M. Brookhart, M. L. H. Green and G. Parkin, *Proc. Natl. Acad. Sci. U. S. A.*, 2007, **104**, 6908–6914.
2   (a) N. Koga, S. Obara, K. Kitaura and K. Morokuma, *J. Am. Chem. Soc.*, 1985, **107**, 7109–7116. (b) L. H. Shultz and M. Brookhart, *Organometallics*, 2001, **20**, 3975–3982.
3   [a] W. E. Piers and J. E. Bercaw, *J. Am. Chem. Soc.*, 1990, **112**, 9406–9407. [b] M. D. Leatherman, S. A. Svejda, L. K. Johnson and M. Brookhart, *J. Am. Chem. Soc.*, 2003, **125**, 3068–3081. [c] M. D. Walter, R. A. Moorhouse, S. A. Urbin, P. S. White and M. Brookhart, *J. Am. Chem. Soc.*, 2009, **131**, 9055–9069.
4   (a) S. H. Crosby, G. J. Clarkson and J. P. Rourke, *J. Am. Chem. Soc.*, 2009, **131**, 14142–14143. (b) D. Balcells, E. Clot and O. Eisenstein, *Chem. Rev.*, 2010, **110**, 749–823. (c) S. Murugesan, B. Stöger, E. Pittenauer, G. Allmaier, L. F. Veiros and K. Kirchner, *Angew. Chem. Int. Ed.*, 2016, **55**, 3045–3048.
5   E. M. Matson, G. Espinosa Martinez, A. D. Ibrahim, B. J. Jackson, J. A. Bertke and A. R. Fout, *Organometallics*, 2015, **34**, 399–407.
6   A. D. Ibrahim, K. Tokmic, M. R. Brennan, D. Kim, E. M. Matson, M. J. Nilges, J. A. Bertke and A. R. Fout, *Dalt. Trans.*, 2016, **45**, 9805–9811.
7   B. J. Jackson, D. C. Najera, E. M. Matson, T. J. Woods, J. A. Bertke and A. R. Fout, *Organometallics*, 2019, **38**, 2943–2952.
8   G. E. . Martinez, J. A. Killion, B. J. Jackson and A. R. Fout, *Inorg. Synth.*, 2018, **37**, 50-55.
9   (a) X. Wang, Z. Mo, J. Xiao and L. Deng, *Inorg. Chem.*, 2013, **52**, 59–65. (b) H. Schneider, D. Schmidt, A. Eichhöfer, M. Radius, F. Weigend and U. Radius, *Eur. J. Inorg. Chem.*, 2017, **2017**, 2600–2616. (c) S. Zhang and J. P. Krogman, *Organometallics*, 2021, **40**, 1926–1933.
10   A. W. Addison, T. N. Rao, J. Reedijk, J. van Rijn and G. C. Verschoor, *J. Chem. Soc., Dalt. Trans.*, 1984, 1349–1356.
11   N. P. Mankad, M. T. Whited and J. C. Peters, *Angew. Chem. Int. Ed.*, 2007, **46**, 5768–5771.
12   This was further corroborated by attempted metalations with *o*-substituted pyridine derivatives, 2,6-lutidine and 2-picoline, which produced intractable mixtures.
13   For a thorough study about the shifts of agostic protons see: J. E. Barquera-Lozada, A. Obenhuber, C. Hauf and W. Scherer, *J. Phys. Chem. A,* 2013, **117**, 4304–4315.
14   B. Cordero, V. Gómez, A. E. Platero-Prats, M. Revés, J. Echeverría, E. Cremades, F. Barragán and S. Alvarez, *Dalton Trans.*, 2008, 2832–2838.
15   (a) Y. Zhang, J. C. Lewis, R. G. Bergman, J. A. Ellman and E. Oldfield, *Organometallics*, 2006, **25**, 3515–3519; (b) D. Braga, F. Grepioni, K. Biradha and G. R. Desiraju, *J. Chem. Soc., Dalton Trans.,* 1996, 3925–3930. (c) D. Himmelbauer, M. Mastalir, B. Stöger, L. F. Veiros, M. Pignitter, V. Somoza and K. Kirchner, *Inorg. Chem.*, 2018, **57**, 7925–7931.
16   (a) J. Contreras-García, E. R. Johnson, S. Keinan, R. Chaudret, J.-P. Piquemal, D. N. Beratan and W. Yang, *J. Chem. Theory Comput*. 2011, 7, 625–632. (b) A similar methodology has been recently used in: Y. J. Park, M. N. Peñas-Defrutos, M. J. Drummond, Z. Gordon, O. R. Kelly, I. J. Garvey, K. L. Gullett, M. García-Melchor and Alison R. Fout, *Inorg. Chem.*, 2022, **61**, 8182-8192.
17   For a related study reported for a set Rh and Ir complexes, see: R. C. Knighton, J. Emerson-King, J. P. Rourke, C. A. Ohlin and A. B. Chaplin, *Chem. Eur. J.,* 2018, **24**, 4927–4938.
18   J. J. Race, A. R. Burnage, T. M. Boyd, A. Heyam, A. J. Martínez-Martínez, S. A. Macgregor and A. S. Weller, *Chem. Sci.,* 2021, **12**, 8832–8843.
19   A. R. Hermes and G. S. Girolami, *Organometallics*, 1988, **7**, 394–401
20   S. Fernández-Moyano, M. N. Peñas-Defrutos, C. Bartolomé and P. Espinet, *Inorg. Chem.*, 2021, **60**, 14410–14417.